© 2017. Published by The Company of Biologists Ltd | Journal of Experimental Biology (2017) 220, 2026-2035 doi:10.1242/jeb.151738

RESEARCH ARTICLE

Living with a leaky skin: upregulation of ion transport proteins during sloughing

Nicholas C. Wu, Rebecca L. Cramp and Craig E. Franklin*

ABSTRACT

Amphibian skin is a multifunctional organ providing protection from the external environment and facilitating the physiological exchange of gases, water and salts with the environment. In order to maintain these functions, the outer layer of skin is regularly replaced in a process called sloughing. During sloughing, the outermost layer of the skin is removed in its entirety, which has the potential to interfere with skin permeability and ion transport, disrupting homeostasis. In this study, we measured, *in vivo*, the effects of sloughing on the cutaneous efflux of ions in toads *Rhinella marina* kept in freshwater conditions. We also measured transepithelial potential, cutaneous resistance, active ion transport and the distribution, abundance and gene expression of the key ion transport proteins sodium–potassium ATPase (NKA) and epithelial sodium channel (ENaC) during sloughing. We hypothesised that the increase in transepithelial efflux of ions during sloughing is a consequence of increased permeability and/or a reduction in the abundance or expression of cutaneous ion transport proteins, resulting in disruption of internal ion homeostasis. There was a significant increase in sodium and chloride efflux during sloughing in *R. marina*. However, although *in vitro* skin resistance decreased after sloughing, active sodium transport increased commensurate with an increase in NKA and ENaC protein abundance in the skin. These changes in skin function associated with sloughing did not affect the maintenance of internal electrolyte homeostasis. These results suggest that during sloughing, amphibians actively maintain internal homeostasis by increasing cutaneous rates of ion uptake.

KEY WORDS: Amphibian, Homeostasis, Moulting, qPCR, Sodium transport, Western blotting

INTRODUCTION

The skin, the largest vertebrate organ, has evolved into a complex, pluri-stratified, multi-membrane system (Lillywhite and Maderson, 1988) with vital, often contrasting, functions (reviewed in Chuong et al., 2002). It must act as an impermeable barrier to protect the organism from environmental stressors (abiotic and biotic) (Proksch et al., 2008) while simultaneously being able to sense, interact and exchange some solutes with the surrounding environment (Hillyard et al., 2007). For amphibians, this is especially important as their skin regulates the exchange of electrolytes, water and respiratory gases with the environment to maintain internal homeostasis (Boutilier et al., 1992; Shoemaker et al., 1992).

School of Biological Sciences, The University of Queensland, Brisbane, QLD 4072, Australia.

*Author for correspondence (c.franklin@uq.edu.au)

C.E.F., 0000-0003-1315-3797

Received 18 October 2016; Accepted 20 March 2017

Histologically, the skin of amphibians consists of an outer multilayered epidermis and an inner dermal layer (dermis). The most basal layer of the epidermis is the stratum germinativum, which is attached to the dermis by a basement membrane. The columnar cells of the s. germinativum continually regenerate (via mitotic division), to replenish and maintain the rest of the epidermal cell population (Heatwole et al., 1994). Above the s. germinativum is the s. spinosum ('spiny layer'), where cellular keratinisation begins. Above the s. spinosum is the s. granulosum (granular layer) where the keratinocytes become known as granular cells. These cells are connected by tight junctions (zonulae occludens) that separate the apical plasma membrane from the basolateral membrane lining the lateral intercellular space (Farquhar and Palade, 1964). The apical plasma membrane of granular cells therefore forms the limiting barrier for transcellular solute and water transport across the epidermis, with connections between this layer and the underlying layers (s. spinosum and s. germanitivum) forming an electrical syncytium. The most superficial layer of the epidermis is the s. corneum, which consists of 1–2 thin layers of dead cells (reviewed in Heatwole et al., 1994).

Because of constant interactions with the external environment, the skin must be renewed in order to maintain functionality (Ling, 1972). All metamorphosed amphibians go through a physiological and behavioural phase known as 'ecdysis' or 'sloughing' (Ling, 1972; Larsen, 1976), where the old s. corneum is removed and replaced periodically with a new layer (derived from the underlying s. granulosum). In the early shedding stage, the old s. corneum becomes separated from the underlying cell layer via a gradual dissolution of the desmosomes between these two layers (Budtz, 1977). The new s. corneum (derived from the underlying s. granulosum) swells, flattens (Ernst, 1973) and becomes cornified (Elias and Shapiro, 1957; Whitear, 1975). Mucus also appears beneath the separated s. corneum (known as a 'slough') to facilitate removal (Larsen, 1976). During the post-shedding phase, the new s. corneum flattens and becomes denser in appearance (Budtz and Larsen, 1973). Fusion of the s. granulosum layer leads to the formation of tight junctions (Budtz and Larsen, 1975), which serve to limit the paracellular movement of salts and water (Tsukita et al., 2001; Niessen, 2007). While sloughing maintains the integrity of the skin, physiological changes have been observed to coincide with sloughing that may disturb homeostatic balance. Jørgensen (1949) first observed an increase in cutaneous permeability in sloughing *Bufo bufo*, *Rana temporaria* and *Rana esculenta* which increased the rate of both water gain and sodium loss. These changes in skin permeability can start 12 h ahead of sloughing (Ewer, 1951), and continue 3–4 h post-sloughing (Jørgensen, 1949).

The temporary disruption of cutaneous integrity that occurs during sloughing corresponds with changes to the skin's electrophysiological properties. During sloughing there is a

Journal of Experimental Biology

Journal of Experimental Biology (2017) 220, 2026-2035 doi:10.1242/jeb.151738

decrease in the short-circuit current (indicative of active ion transport activity), transepithelial potential (indicative of the electrical potential difference between the two sides of the cell membrane) and skin resistance (Larsen, 1970, 1971a; Nielsen and Tomilson, 1970). These changes seem to result from the physical shedding of the slough, as they are initiated by the separation of the slough from the underlying skin layer (reviewed in Erlij and Ussing, 1978). However, these studies artificially induced sloughing through the administration of hormones such as aldosterone (Nielsen, 1969; Larsen, 1971a), which can potentially create unrealistic electrophysiological data (relative to natural or spontaneous sloughing), because aldosterone also acts to regulate ion and water reabsorption in the kidneys (Garty, 1986; Eaton et al., 2001) and skin (Bentley, 2002), and increases protein synthesis in the bladder and skin (Crabbé and de Weer, 1964). Thus, many of these earlier sloughing studies are difficult to interpret, as the observed electrophysiological changes of the skin may be an artefact of aldosterone administration instead of the natural physiological changes that occur during sloughing.

While earlier studies have suggested that the physical alterations that occur to amphibian skin during sloughing (e.g. removal of tight junctions) cause the increase skin permeability (Smith, 1975; Larsen, 1976), Katz (1978) suggested disruption of tight junctions was not solely responsible for the observed changes in specific permeability of the skin to Na^+ and K^+ during sloughing. A reduction in the abundance or activity of transepithelial ion transport proteins such as epithelial sodium channels (ENaC) or the sodium–potassium pump (Na^+/K^+-ATPase; NKA) during sloughing may also cause disruption to the transportation of ions. ENaC is a membrane-bound protein channel found in the apical membrane of epithelial cells that is responsible for the uptake of Na^+ from the environment, while NKA is an active membrane protein pump found in the basolateral layer of epithelial cells that establishes an electrochemical gradient for ion channels like ENaC to transport Na^+ against their concentration gradients (Hillyard et al., 2008). Thus, examining the relative expression of these proteins in sloughing amphibians relative to non-sloughing amphibians may clarify the mechanism through which this disruption of ion transport during sloughing occurs.

To date, there is no direct link with the activities of the epithelial transport proteins and the changes in ion and osmotic transport during sloughing. As there are physical and physiological changes in the skin associated with sloughing (Larsen, 1976; Erlij and Ussing, 1978), does the change in skin function cause temporary electrolyte disruption in the animal's homeostasis (e.g. blood biochemistry), or does the skin actively upregulate expression of epithelial ion transporters (e.g. ENaC and NKA) to maintain homeostasis? Taking an integrative approach, this study aimed to investigate the effects of sloughing on epidermal ion transport *in vivo* and *in vitro*, the distribution, abundance and expression of associated regulatory transport proteins, and blood plasma biochemistry in cane toads, *Rhinella marina* (Linnaeus 1758). This study also avoided the influence of hormone-induced sloughing by investigating epithelial transport in spontaneously sloughing anurans.

We hypothesised that as a result of physical changes to the skin during spontaneous sloughing there would be disruption of cutaneous ion and water transport (Jørgensen, 1949), with a reduction in the abundance and expression of ion transport proteins (e.g. ENaC and NKA), resulting in a transient disruption to internal ion and water homeostasis.

MATERIALS AND METHODS

Animal maintenance

Rhinella marina (n=24) were collected from The University of Queensland campus, Brisbane, Australia, between November 2014 and January 2015, and housed in large black bins (n=5 per bin) containing a thin layer of pine-bark mulch (Richgro, WA, Australia). Toads were checked daily, fed weekly on vitamin-dusted (Aristopet Pty Ltd, QLD, Australia) crickets (*Acheta domesticus*), and enclosures were cleaned weekly. After approximately 2 weeks, toads were housed individually in ventilated polypropylene plastic containers (130×140×325 mm) with a thin layer of pine-bark mulch saturated with tap water, which were tilted to allow a wet and dry gradient for the toads to move between. All toads were kept at 25±0.3°C on a 12 h:12 h light:dark cycle. All procedures in this study were carried out with the approval of The University of Queensland's Animal Ethics Unit (approval no. SBS/316/14/URG).

Monitoring sloughing frequency

To determine sloughing events, *R. marina* (n=24) were marked with a small amount of non-toxic waterproof zinc cream (Key-Sun Laboratories, NSW, Australia) on the dorsal surface following Meyer et al. (2012). Animals were checked twice daily to record the disappearance of the marks as an indication of sloughing. Once a mark disappeared, it was reapplied. The time (in days) between mark application and loss was recorded as the intermoult interval (IMI). The sloughing behaviour for *R. marina* was divided into four stages: (1) intermoult, the period in between each slough; (2) pre-sloughing, when animals started to extend their limbs to lift the abdomen off the ground; (3) sloughing, which begins with mouth gaping, followed by abdominal contractions, upper body wiping and removal of the old skin; and (4) post-sloughing, up to 1 h after sloughing when normal behaviour resumes.

Electrolyte conductivity

To measure changes in *in vivo* ion efflux during sloughing, each animal was placed in an open-ended ventilated clear chamber (75×110×160 mm) containing 300 ml of reverse osmosis water with a magnetic stirrer to circulate the solution. The rate of ion efflux was measured as the change in conductivity (in $\mu S\ h^{-1}$) for toads in each of the following moult stages: (1) intermoult, (2) pre-sloughing, (3) sloughing and (4) post-sloughing (Fig. 1) for 9 animals. A conductivity electrode connected to a conductivity pod (ML307, ADInstruments, NSW, Australia) was placed at each end of the chamber. The output was digitised with a PowerLab 4/35 interface (ADInstruments) and recorded on Labchart software (ADInstruments). The baseline of the bathing solution was measured (average from the two electrodes) for roughly an hour before the animal was placed into the chamber (Fig. 1). A change in the conductivity of the bathing solution associated with sloughing was determined via video surveillance, and duration of the sloughing event (min) was recorded. The experiment was conducted at room temperature (22±0.5°C). Animals were fed weekly, but because of the difficulty in determining when animals would slough (7 day variation), animals were not fasted prior to measurements and may have been in different digestive states. Both fasted and recently fed animals were included in the analysis as there was no significant difference in the rate of conductivity (t_{50}=−0.76, P=0.45) between fasted and recently fed animals.

The net loss of Na^+ and K^+ into the bathing solution was measured using flame photometry (BWB-XP flame photometer, BWB Technologies Ltd, UK). The net loss of Cl^- was determined

Journal of Experimental Biology (2017) 220, 2026-2035 doi:10.1242/jeb.151738

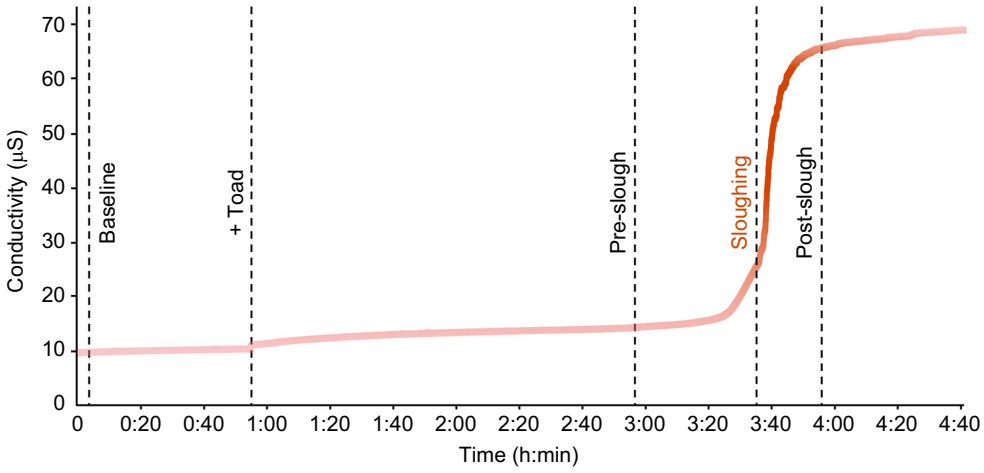

Fig. 1. Example raw trace of changes in conductivity readings associated with sloughing for one cane toad, *Rhinella marina*. Body mass (M_b)=46.7 g, snout–vent length (SVL)=86 mm. 'Baseline' values were obtained from the chamber water in the absence of animals; '+Toad' data were obtained with the animal inside the experimental chamber.

spectrophotometrically (DTX 880 Multimode Detector, Beckman Coulter, IA, USA) using a commercially available chloride kit according to the manufacturer's instructions (MAK023, Sigma-Aldrich, MO, USA). The conductivity readings (µS h^{-1}) were converted to NaCl efflux (mmol l^{-1}) using known concentrations of NaCl solutions (0–1 mmol l^{-1}). The conductivity readings of the solution and known NaCl concentrations showed a predictable linear relationship (r^2=0.99; Fig. S1). To estimate the overall effect of sloughing on the total sodium content of the extracellular fluid (ECF), conductivity measures were converted to a rate of sodium loss (mmol h^{-1}) based on [Na^+] of bath water samples collected after sloughing and assuming that sodium was the primary ion contributing to solution conductivity and that there was an equal proportion of sodium lost relative to other ions. The net amount of Na^+ lost during sloughing was calculated assuming an ECF volume of approximately ∼25% of the body mass of the animal (Thorson, 1964). The actual Na^+ concentration of the ECF was measured from plasma samples (see below). The proportion of the total ECF Na^+ (as a percentage of ECF Na^+ h^{-1}) lost during sloughing was calculated by dividing the rate of ion loss (mmol l^{-1} h^{-1}) by the total amount of ECF Na^+ (mmol) multiplied by 100.

Before and after each conductivity trial, animals were voided of urine by gently applying pressure on the ventral side. Body mass (M_b; g) was then measured (Adam Equipment Co. Ltd, CT, USA) to calculate any change over the sloughing period as percentage change in M_b per hour. The change in M_b over the tested interval represents osmotic water flux. Animals that urinated or defected during the experiment were taken out and re-weighed before being returned to the chamber, with fresh bathing solution.

Blood plasma biochemistry

Toads (n=14 intermoult, n=10 post-sloughing) were killed via double pithing at one of two time points: (1) post-sloughing (no more than 1 h after sloughing had occurred), or (2) intermoult (at a point halfway through the IMI). Snout–vent length (SVL) and M_b were measured immediately. Blood was collected via cardiac puncture into a lithium heparinised syringe. Samples were then centrifuged at 5000 ***g*** for 5 min and the plasma collected and stored at −20°C for subsequent electrolyte analysis. Two heparinised capillary tubes of whole blood were also centrifuged at 5000 ***g*** for 3 min to determine haematocrit (Hct). Plasma Na^+ and K^+ levels (mmol l^{-1}) were measured using flame photometry, and plasma osmolality (mosmol l^{-1}) was measured using a Vapro 5520 vapour pressure osmometer (Wescor, Logan, UT, USA). Plasma Cl^- levels (mmol l^{-1}) were determined spectrophotometrically (DTX 880 Multimode Detector, Beckman Coulter, IA, USA) using a chloride kit according to the manufacturer's instructions (MAK023, Sigma-Aldrich).

Electrophysiology of the ventral skin

Ventral skin samples (<1 cm^2, intermoult n=8, post-sloughing n=8) were collected from the lower abdominal pelvic patch region of animals used for blood biochemistry analyses (see above), and mounted in a self-contained, single-channel Ussing chamber apparatus (model U-9926, Warner Instruments, Hamden, CT, USA) with a single-channel epithelial voltage-clamp amplifier (model EC-800, Warner Instruments). Apical and basolateral surfaces of the skin were perfused with an oxygenated (95% O_2 and 5% CO_2) frog Ringer solution (mmol l^{-1}: NaCl 112, KCl 2.5, D-glucose 10, Na_2HPO_4 2, $CaCl_2$ 1, $MgCl_2$ 1, Hepes salt 5, Hepes 5, at pH 7.4 with an osmolality of 230±20 mosmol l^{-1}; Voyles et al., 2009), and temperature was maintained via a water bath set at 25±1°C. Electrophysiological parameters were measured as follows: (1) transepithelial potential (V_T) under open-circuit conditions by clamping the current to 0 µA and recording the resulting voltage (mV) with reference to the basolateral side, (2) active ion transport via clamping the voltage to 0 mV and recording the instantaneous short-circuit current (I_{sc}) response (µA cm^2) and (3) transepithelial resistance per unit area (Ω cm^{-2}) by applying 3 s of 1 µA pulses across the epithelium every 60 s, or under voltage-clamp conditions by applying 3 s of 1 mV at 60 s intervals (Ruhr et al., 2014). The inflections from the resulting change in I_{sc} and V_T during pulsing were used to calculate resistance using Ohm's law. Sodium flux was calculated by dividing the I_{sc} by Faraday's constant using the following formula:

$$J_{Na} = \frac{I_{sc}}{F}, \quad (1)$$

where J_{Na} is the sodium flux (mol s^{-1}), I_{sc} is the short-circuit current (µA) and F is Faraday's constant (96,485 C mol^{-1}). The relationship between flux and current is the same as that between concentration and charge (Ussing and Zerahn, 1951). Thus, a current measured in µA corresponds to a net transport rate of 10^{-11} mol s^{-1}.

The transepithelial potential and resistance were also measured under more ecologically realistic conditions consistent with 'freshwater' on the apical skin side (26 mmol l^{-1} NaCl in distilled water), where the electrochemical gradient across the skin would

favour a net efflux of ions during sloughing. The traditional approach of using Ringer solution on both surfaces of the membrane could potentially negate this condition.

Histological analysis of epithelial transport proteins

Epidermal thickness was compared between intermoult and post-sloughing toads. Ventral skin samples (<1 cm^2) from the lower abdominal pelvic patch region were collected and placed into aqueous buffered zinc formalin fixative (Z-fix, Anatech, MI, USA) for 24 h, then transferred to 70% ethanol and stored at 4°C. Tissue samples (intermoult n=6, post-sloughing n=6) were then dehydrated through an ascending ethanol series, cleared in xylene and embedded in paraffin wax (Histoplast Paraffin, ThermoFisher Scientific, Sydney, Australia). Tissue samples were then transversely sectioned into approximately 6 µm-thick sections (Leica RM2245, Leica Microsystems, NSW, Australia), stained with Mayer's haematoxylin and 1% eosin in 70% ethanol, and photographed with NIS-Elements software (v. 4.10, Nikon Instruments Inc., Tokyo, Japan) under bright-field illumination (Nikon Eclipse E200 MV, Nikon Instruments Inc.).

NKA distribution

Distribution of the NKA α-subunit in the ventral skin tissues was examined via immuno-fluorescence staining. Distribution of the ENaC α-subunit in skin sections was not examined as the antibody (Anti-SCNN1A antibody, HPA012939, Sigma-Aldrich) did not function well in our immunohistochemistry protocol. Sections were de-paraffinised then washed in washing buffer (0.01 mol l^{-1} PBS, 0.05% Tween-20, pH 7.4; 2×3 min washes) and blocked at room temperature in normal goat serum (2% goat serum, 1% BSA, 0.1% cold fish skin gelatine, 0.1% Triton X-100, 0.05% Tween-20 and 0.05% thiomerosal in 0.01 mol l^{-1} PBS, pH 7.4). Sections were then incubated in a humidified chamber overnight at 4°C with the NKA primary antibody α5 (developed by the Developmental Studies Hybridoma Bank, created by the NICHD of the NIH, and maintained at The University of Iowa, Department of Biology), diluted 1:500 in 1% BSA, 0.1% cold fish skin gelatine and 0.05% thiomerosal in 0.01 mol l^{-1} PBS. Subsequently, sections were incubated with a fluorophore-conjugated secondary antibody (goat anti-mouse IgG Dylight, ab96879, Abcam Inc., Cambridge, UK) diluted 1:500 in 0.01 mol l^{-1} PBS and 0.05% Tween-20 for 1 h in the dark at room temperature. They were then mounted with Fluoroshield DAPI mounting medium (Sigma-Aldrich), and viewed using a Nikon Eclipse E200 MV series epi fluorescence microscope and photographed using NIS-Elements software.

Ion transporter abundance

Semi-quantitative Western blotting was performed to estimate the relative abundance of NKA α-subunit and ENaC α-subunit in the ventral skin tissues of intermoult (n=4) and post-sloughing (n=4) toads. Ventral skin samples (<1 cm^2) from the lower abdominal pelvic patch region were collected and stored at −80°C. Frozen tissues were then homogenised in ice-cold membrane extraction homogenisation buffer [250 mmol l^{-1} sucrose, 30 mmol l^{-1} Tris, 1 mmol l^{-1} EDTA, 100 µg ml^{-1} phenylmethylsulfonyl fluoride (PMSF) and 5 mg ml^{-1} protease inhibitor cocktail], and centrifuged at 1200 ***g*** for 15 min at 4°C. The supernatant was then removed and centrifuged at 23,000 ***g*** for 25 min at 4°C. The resulting pellet was re-suspended in 50 µl of homogenisation buffer. An aliquot was used for Bradford protein quantification (Sigma-Aldrich).

A 5 µg sample of total membrane protein in NuPAGE LDS sample buffer (Invitrogen) was loaded in triplicate into Bolt 4–12% Bis-Tris Plus gels (ThermoFisher Scientific) and electrophoresed at 140 V for 1 h. Gels were subsequently transferred onto 0.45 µm Westran PVDF blotting membranes (Sigma-Aldrich) at 20 V for 75 min. Membranes were then blocked in blocking buffer [5% skim milk in TBST (20 mmol l^{-1} Tris, 150 mmol l^{-1} NaCl and 1% Tween-20, pH 7.6)] for 1 h at room temperature before incubation overnight at 4°C with their respective primary antibody [0.2 µg ml^{-1} NKA primary antibody α5 and 0.15 µg ml^{-1} ENaC α-subunit primary antibody (Anti-SCNN1A antibody, HPA012939, Sigma-Aldrich)] diluted in blocking buffer. Membranes were then incubated in secondary goat anti-mouse IgG horseradish peroxide (HRP)-conjugated antibody (1.2 µg ml^{-1}; C22P20, Antibodies Australia, VIC, Australia) and goat anti-rabbit IgG HRP-conjugated antibody (0.6 µg ml^{-1}; C24P03, Antibodies Australia), respectively, for 1 h at room temperature, and stained with 1-Step Ultra TMB-Blotting solution (ThermoFisher Scientific). The membranes were dried and digitised for densitometry analysis with Image J (https://imagej.nih.gov/ij/). The pixel densities were used to estimate protein abundance in the post-sloughing animals, expressed relative to the intermoult group.

Ion transporter expression

RNA extraction and cDNA synthesis

Ventral skin samples (<1 cm^2) from the lower abdominal pelvic patch region were collected and stored in RNA-later (Ambion Inc., TX, USA) at −20°C. The skin samples were homogenised with stainless steel beads using a TissueLyser II (Qiagen). Total RNA was isolated using an RNeasy Mini kit with on-column DNAse treatment as per the manufacturer's guidelines (RNeasy Mini kit, Qiagen, Hilden, Germany). RNA purity was assayed by spectrometry, and yield measured using a Qubit fluorometer (ThermoFisher Scientific). RNA was then reverse transcribed into cDNA (SensiFAST™ cDNA synthesis kit, Bioline, NSW, Australia), with appropriate controls (no reverse transcriptase), followed by RNase H treatment.

Primer design and quantification of mRNA by quantitative PCR

Quantitative PCR (qPCR) primers against the target gene ENaC (*scnn1a*, sodium channel epithelial 1 alpha subunit) and the housekeeping gene glyceraldehyde 3-phosphate dehydrogenase (*GAPDH*) were manufactured using previously published species-specific primer sequences (Konno et al., 2007). Species-specific primers against the target gene NKA (*atp1a1*, ATPase Na^+/K^+ transporting subunit alpha 1) were designed from published *R. marina* NKA-α1 subunit sequence (GenBank: Z11798.2; Jaisser et al., 1992) using OligoPerfect™ Designer (ThermoFisher) with acceptance of the default parameters. qPCR was performed using the SensiFAST™ SYBR No-ROX kit (Bioline, NSW, Australia) in a thermal cycler (MiniOpticon™, Bio-Rad) using the cycling parameters recommended in the qPCR kit. Each assay (in triplicate) included a no-template control and a no-reverse transcriptase control. All PCR efficiencies were >90% and all the assays produced unique dissociation curves. Bio-Rad CXF Manager software (version 3.1, Bio-Rad) results were exported as tab-delimited text files and imported into Microsoft Excel for further analysis. The expression of each gene was quantified relative to the expression of *GAPDH* using the Pfaffl (2001) method.

Statistical analysis

All analyses were performed in R.3.0.1 (https://CRAN.R-project.org/package=nlme). Data were presented either as means±s.e.m. or as individual data points depending on the nature of the data (Cumming et al., 2007; Krzywinski and Altman, 2013), and α was set at 0.05 for all statistical tests.

Journal of Experimental Biology (2017) 220, 2026-2035 doi:10.1242/jeb.151738

Electrolyte conductivity

Differences in the rate of conductivity between each group were analysed using linear mixed effects (lme) models in the R 'nlme' package (https://CRAN.R-project.org/package=nlme) with groups (intermoult, pre-sloughing, sloughing, post-sloughing) as fixed effects, M_b (g) as covariate, and individual identity as a random effect to account for repeated measurements within individuals. Changes in M_b (M_b before – M_b after) following the *in vivo* ion loss experiment between intermoult and sloughing groups were analysed using linear mixed effects (lme) models with group (intermoult, post-sloughing) as fixed variable, duration in the experiment as covariate, and individual identity as a random effect to account for repeated measurements within individuals.

Blood plasma biochemistry and electrophysiology of the skin

Differences between the intermoult and post-sloughing group in plasma biochemistry (Hct, Na^+, K^+, Cl^- and osmolality), and the electrophysiological properties of the skin (transepithelial potential, resistance and active transport) were analysed by analysis of covariance (ANCOVA) with time (h) of post-mortem blood and skin tissue collection as covariates.

ENaC and NKA abundance and gene expression

Differences in staining intensity of antibody bands representing NKA α-subunit and ENaC α-subunit relative abundance and relative expression of NKA and ENaC between intermoult and post-sloughing groups were compared using ANCOVA with group (intermoult and post-sloughing) as fixed effect and time (h) of post-mortem skin tissue sample collection as covariate.

RESULTS

Moulting behaviour

The IMI of *Rhinella marina* held at 25°C was variable within and between individuals and ranged from 5 to 16 days with a mean of 10.5±1.8 days (n=24). There was no diurnal effect on sloughing, with 53% of toads sloughing at night and 47% during the day. The IMI tended to be longer in larger toads (t_{19}=−2, P=0.051, n=24).

Ion efflux and water influx during sloughing

The average rate of change in conductivity in the bathing water, representing ion efflux rate from toads, increased 160 times (t_{48}=27.7, P<0.0001; Fig. 2A) from 0.5±0.1 µS h^{-1} in intermoult animals to 90±6.9 µS h^{-1} during sloughing. An increase in conductivity was also recorded just prior to sloughing (11.5± 1.0 µS h^{-1}; t_{48}=3.2, P=0.002). The rate of efflux of ions returned to baseline levels rapidly (within 30 s; Fig. 1) after sloughing (t_{48}=0.67, P=0.5). The majority of the ions lost by the toads were sodium and chloride. The estimated net loss of Na^+ during the hour incorporating the sloughing event represented ∼3.3±0.5% of the animal's total ECF Na^+ pool.

There was no significant difference in the net change in mass between those that sloughed (0.2±0.3% h^{-1}) and the intermoult group (−0.4±0.6% h^{-1}) during the conductivity measurements (t_{22}=−0.01, P=0.99; Fig. 2B), and the duration of sloughing also had no effect on the change in M_b between treatments (t_{30}=1.16, P=0.25).

Electrophysiological properties of the skin

There was no significant difference in the transepithelial potential (mV) and resistance (Ω cm^2) between the intermoult and post-sloughing groups when the toad skin was perfused with Ringer solution on both sides (Table 1). However, the post-sloughing group showed a significant increase in I_{sc} (15.4±2.7 µA cm^{-1}) compared with the intermoult group (8.0±0.9 µA cm^{-1}; Table 1). This represents a rate of active Na^+ transport (influx) of $1.6\times10^{-10}\pm3.2\times10^{-11}$ mol s^{-1} after sloughing.

When the skin was perfused with freshwater on the apical side of the chamber, the transepithelial potential did not differ significantly between the intermoult and post-sloughing group (Table 1); however, there was a significant decrease in transepithelial resistance in the post-sloughing group compared with the intermoult group (Table 1).

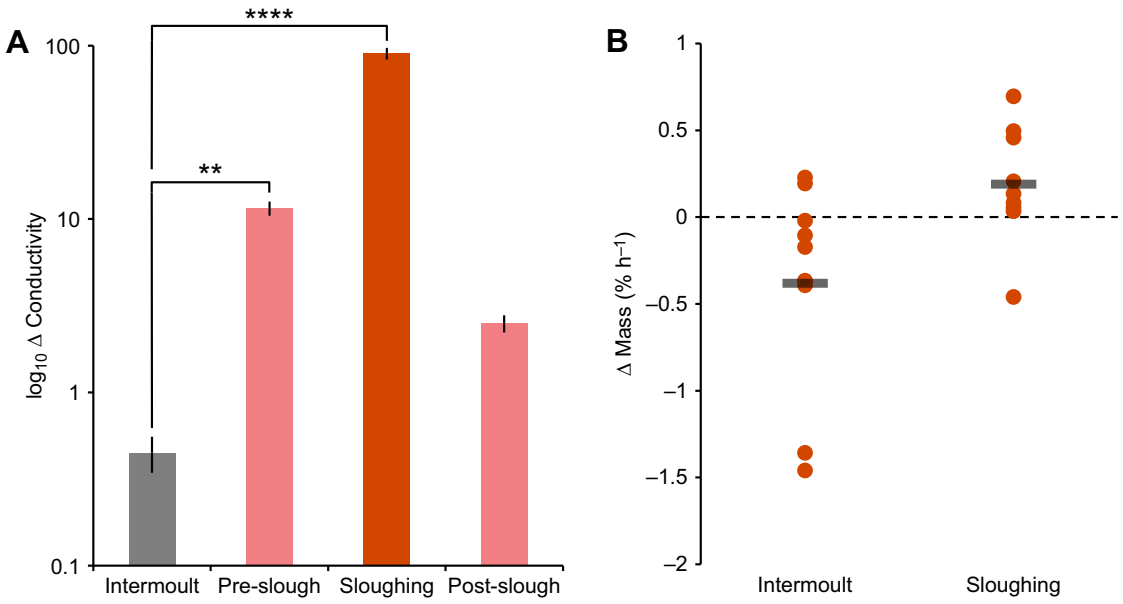

Fig. 2. Change in rate of conductivity and M_b of *R. marina* during sloughing. (A) Rate of change in conductivity (µS h^{-1}) represented on a logarithmic scale between intermoult, pre-sloughing, sloughing and post-sloughing group. Data are means±s.e., **P<0.01 and ****P<0.0001. (B) Change in M_b (% h^{-1}) in the conductivity experiment between the intermoult and sloughing group. Data are presented as individual points of the mean change in mass (circles) with the overall mean represented as a black line. n=9 for intermoult, pre-sloughing, sloughing and post-sloughing groups.

Journal of Experimental Biology

Journal of Experimental Biology (2017) 220, 2026-2035 doi:10.1242/jeb.151738

Table 1. Electrophysiological properties of cane toad (*Rhinella marina*) epidermis between the intermoult and post-sloughing group

	Intermoult		Post-sloughing		
	n	Mean±s.e.	*n*	Mean±s.e.	ANCOVA
Epidermal electrophysiological parameters					
Transepithelial potential (mV)	8	−5.5±0.6	8	−3.9±0.7	$F_{1,13}$=1.9, P=0.2
Resistance (Ω cm^2)	8	3029±433	6	2678±726	$F_{1,11}$=0.15, P=0.7
Short-circuit current (μA cm^{-2})	8	8±0.9	8	15.4±2.7	$F_{1,13}$=6.2, P=0.03
Sodium flux (mol s^{-1})	8	$8.3\times10^{-11}\pm9.5\times10^{-12}$	8	$1.6\times10^{-10}\pm3.2\times10^{-11}$	
Apical freshwater treatment					
Transepithelial potential (mV)	6	−13.2±2.4	8	−19.6±2	$F_{1,11}$=3.4, P=0.09
Resistance (Ω cm^2)	8	12,219±1771	6	6349±1955	$F_{1,11}$=5.4, P=0.04

Apical freshwater treatment represents the apical side of the epidermis containing 26 mmol NaCl in distilled water. *n*=sample size.

Blood plasma biochemistry

Hct, plasma osmolality, and sodium, chloride and potassium concentrations were not significantly different between the intermoult and post-sloughing animals (Table 2).

Skin thickness

There were no significant differences in skin thickness between the intermoult and post-sloughing groups (t_8=−0.99, P=0.34; Fig. 3). No morphological differences were observed between the groups.

ENaC α-subunit and NKA α-subunit protein distribution, abundance and gene expression

The NKA α-subunit was mostly distributed in the epidermis, with little or no immunofluorescence staining in the dermis layer (Fig. 4). The submucosal glands within the skin also showed strong NKA α-subunit immunofluorescence in both intermoult and post-sloughing animals. Within the epidermal layer, the NKA α-subunit was concentrated around the basolateral membranes in the principal cell layer (excluding the s. corneum). NKA α-subunit distribution in the epidermis of all intermoult animals remained relatively uniform (Fig. 4A). In the post-sloughing group, however, NKA α-subunit distribution within the epidermis was less well defined. In some animals, NKA α-subunit distribution was concentrated in the most superficial layers of the epidermis, while in other animals the NKA α-subunit appeared to be restricted to cells in the basal layers of the epidermis (Fig. 4B).

Semi-quantitative western blotting for the NKA α-subunit (α5 antibody) identified a single band of approximately 100 kDa from membrane-enriched skin cell homogenates. NKA α-subunit abundance was significantly higher ($F_{1,12}$=9.5, P=0.009) in the post-sloughing group relative to the intermoult group (Fig. 5). The ENaC α-subunit antibody identified a single band of approximately 75 kDa. The ENaC α-subunit abundance was also significantly greater ($F_{1,12}$=8.8, P=0.01) in the post-sloughing group compared with the intermoult group (Fig. 5), with up to a 2.5-fold increase in abundance occurring in some animals (mean=1.62±0.16).

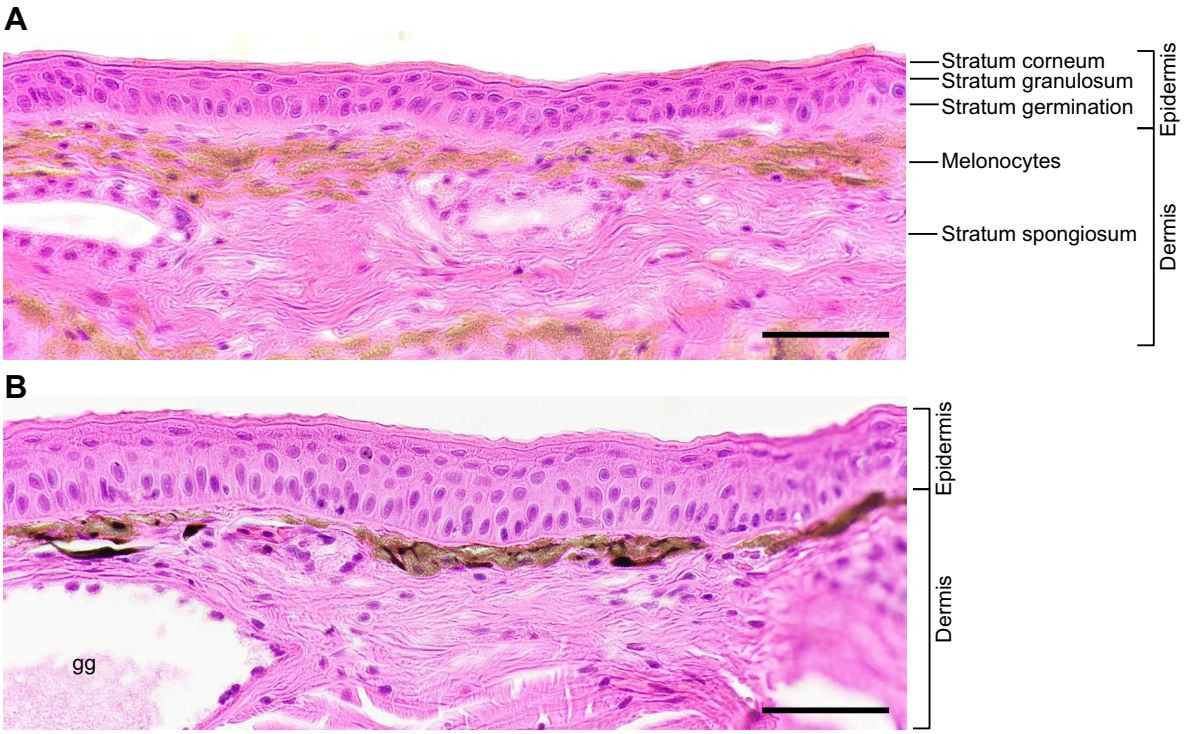

Fig. 3. Differences in the thickness of the epidermis between intermoult and post-sloughing *R. marina*. Transverse section (6 μm) of haematoxylin and eosin (H&E)-stained ventral skin. Average epidermal thickness of (A) 27.2±5.83 μm from an intermoult toad (SVL 106 mm) and (B) 39.2±5.83 μm from a post-sloughing toad (SVL 107 mm). gg, granular gland. Scale bar: 50 μm. EXIF data: *f*/2.2, ISO-32, exposure time 1/50 s.

Journal of Experimental Biology

Journal of Experimental Biology (2017) 220, 2026-2035 doi:10.1242/jeb.151738

Table 2. Comparison of cane toad (*R. marina*) blood plasma biochemistry between the intermoult and post-sloughing group

	Intermoult		Post-sloughing		
Blood biochemical parameters	*n*	Mean±s.e.	*n*	Mean±s.e.	ANCOVA
Haematocrit (%)	14	19.8±1.6	10	23.5±3.7	$F_{1,21}$=0.9, P=0.34
Sodium (mmol l^{-1})	11	116±3.3	10	113±2.6	$F_{1,18}$=0.6, P=0.45
Chloride (mmol l^{-1})	10	92±6.3	9	80±4.8	$F_{1,16}$=1.8, P=0.2
Potassium (mmol l^{-1})	11	3.3±0.1	10	3.4±0.1	$F_{1,18}$=0.5, P=0.47
Osmolality (mosmol l^{-1})	11	236±6.2	10	241±8.4	$F_{1,18}$=0.2, P=0.65

The relative expression of NKA (ATP1A1) and ENaC (SCNN1A) mRNA transcripts in the epidermis was not significantly different between the intermoult and post-sloughing group (Pfaffl ratio: 1.137, $F_{1,5}$=0.06, P=0.8 and Pfaffl ratio: 2.14, $F_{1,5}$=2.5, P=0.1, respectively; Fig. 6).

DISCUSSION

Amphibian skin is a complex multifunctional organ, with the ability to actively regulate the transcutaneous movement of ions and water necessary for maintaining physiological homeostasis (Feder and Burggren, 1992). Understanding the impact of sloughing on skin function is important to comprehend how amphibians maintain homeostatic balance in the face of frequent and significant perturbations. The present study demonstrates that during sloughing, amphibians in freshwater environments are able to compensate for an increase in the rate of transcutaneous sodium loss by increasing the abundance of sodium transporters in the skin, which in turn allows amphibians to maintain their internal electrolyte homeostasis. These findings suggest that although sloughing causes an acute change in skin osmotic function, the effects are relatively transient and are offset by compensatory pathways. How sloughing may impact species with more frequent sloughing regimens or those with disease-related sloughing dysfunction, however, remains to be determined.

Sloughing-associated skin disturbances began ahead of the physical act of sloughing; indeed, there was a 10-fold increase in the rate of ion efflux in live toads prior to the initiation of sloughing. This finding is consistent with previous studies showing that changes in the electrophysiological properties of amphibian skin often precede the physical sloughing event. Specifically, a decrease in I_{sc} has been observed during the initiation of sloughing (*in vitro*) in *B. bufo* (Larsen, 1970, 1971a,b). In isolated amphibian skin, I_{sc} is predominately linked to active sodium uptake (Koefoed-Johnson and Ussing, 1958). A reduction in I_{sc} across the skin during sloughing therefore probably reflects a reduction in active transcutaneous sodium movement. The mechanistic basis for this pre-sloughing change in ion transport remains unclear; however, preparatory shifts in cellular differentiation within the epidermis have been hypothesised to contribute to the observed changes in electrical readings in pre-sloughing amphibians (Larsen, 1971b). Potentially, cellular apoptosis in the s. granulosum as a consequence of its transition to the s. corneum (Elias and Shapiro, 1957) may degrade the ion regulatory transporters responsible for maintaining the potential difference across the skin. This reduction in transporter abundance or activity would lower active sodium uptake rates and contribute to the net increase in sodium loss across the skin. Coincidently, an increase in cutaneous granular secretions to form the mucus layer during sloughing may also contribute to ion loss (Larsen and Ramløv, 2013).

Although some physiological changes preceded sloughing, by far the greatest disruption to skin function in *R. marina* occurred during sloughing itself. Sloughing substantially increased the rate of cutaneous ion efflux in *R. marina*, indicating that skin function

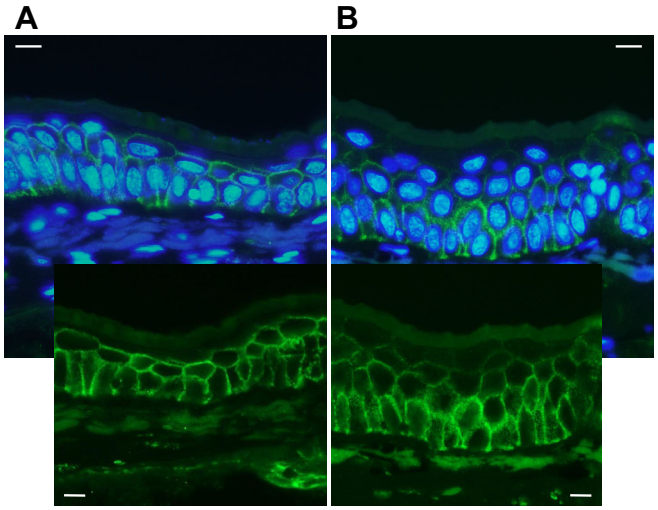

Fig. 4. Differences in Na^+/K^+-ATPase (NKA) distribution between intermoult and post-sloughing *R. marina*. Immunofluorescence staining of NKA α-subunit (green) in transverse sections (6 µm) of ventral skin. (A) Bottom image: NKA distribution within the epidermis of an intermoult animal (SVL 106 mm) remains uniform throughout the epidermis. (B) Bottom image: NKA distribution is concentrated in the basolateral area of the epidermis in a post-sloughing animal (SVL 107 mm). Cellular nuclear DNA was counterstained in DAPI (blue, top). Scale bar, 10 µm.

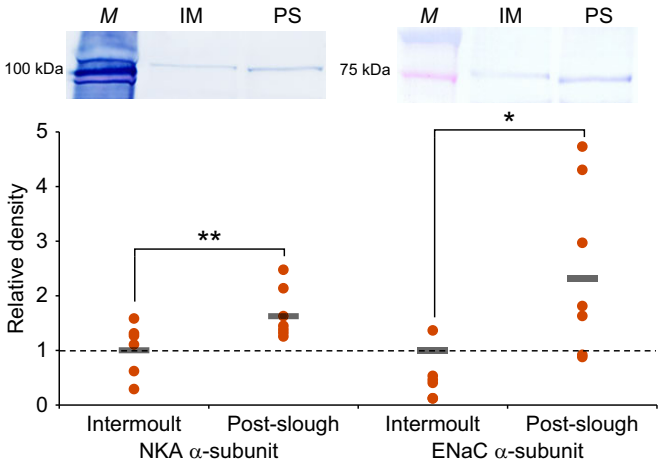

Fig. 5. Relative abundance of NKA α-subunit and epithelial sodium channel (ENaC) α-subunit in ventral epidermal tissues of intermoult and post-sloughing *R. marina*. Individual data points are presented as the mean of three technical replicates of NKA α-subunit (intermoult n=7, post-sloughing n=8) and ENaC α-subunit (intermoult n=7, post-sloughing n=8).The black line indicates the overall mean. Representative western blots associated with each transport protein (top) show the molecular mass (*M*), an intermoult animal (IM) and a post-slough animal (PS). *P<0.05 and **P<0.01.

Journal of Experimental Biology

Journal of Experimental Biology (2017) 220, 2026-2035 doi:10.1242/jeb.151738

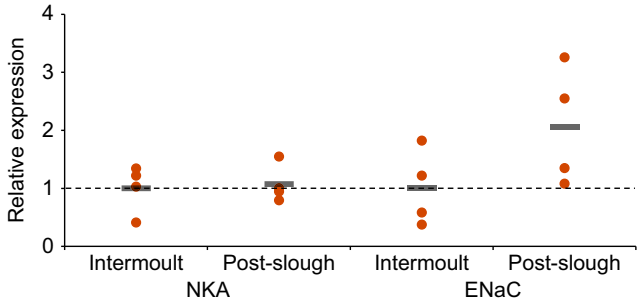

Fig. 6. Comparison of NKA and ENaC mRNA relative expression in ventral epidermal tissues of intermoult and post-sloughing *R. marina*. Absolute gene expression (ΔC_T) was normalised to expression of the housekeeping gene *GAPDH*. Individual data points are presented as the mean of three technical replicates for each ion transporter (n=4). The black line indicates the overall mean.

(specifically active ion transport) was temporarily disrupted during sloughing. In addition, contributing to this net increase in Na^+ efflux, the electrical resistance across the skin was significantly lower in post-sloughed toads, indicating that paracellular resistance to passive ion movements was substantially lower across newly sloughed skin. This reduction in cutaneous resistance following sloughing may be attributed to incompletely formed tight junctions in the new s. granulosum layer (Budtz and Larsen, 1975) that permits the passive paracellular movement of ions out of the animal along their concentration gradient (Larsen, 1970, 1971b, 1972). In *B. bufo*, the reduction in skin resistance can be observed a few hours before the initiation of sloughing (Larsen, 1970, 1971b), suggesting the process of epidermal renewal and formation of the new s. corneum increases the skin's permeability before sloughing (Budtz and Larsen, 1975).

Despite the increased loss of Na^+ preceding and during sloughing, toads were able to maintain osmoregulatory homeostasis with no changes in plasma solute concentration or osmolality detected post-sloughing. This indicates that either the transient nature of the sloughing-induced changes are not substantial enough to disrupt whole-animal ionic homeostasis or active mechanisms are employed during or shortly after sloughing to counteract or compensate for ionic and osmotic fluxes. Jørgensen (1949), using *in vitro* measures of NaCl loss, estimated that the overall amount of Na^+ lost during a sloughing cycle probably reflects a relatively small component of a healthy, normal animal's extracellular sodium pool, consistent with the small net sodium loss measured in this study. Compensatory changes to ion transport may include a change in the activity or abundance or ion transporters in the skin that allow sodium to be actively taken up across the skin from the environment. Consistent with this hypothesis, we observed a 2-fold increase in the I_{sc} across the skin of recently sloughed *R. marina*, suggestive of an increase in active sodium transport. Moreover, we observed a greater abundance of cutaneous ion transporter proteins (NKA α-subunit and ENaC α-subunit) in recently sloughed toads, suggesting that the increase in active sodium transport may, at least in part, be ascribed to an increase in the number of functional sodium transport proteins in the skin. However, the I_{sc} (the likelihood of the number of channels opened at a particular time) alone cannot determine the functional activity of ENaC, as the open probability is highly variable depending on external factors (Anantharam et al., 2006; Kleyman et al., 2009); thus, measuring amiloride-sensitive I_{sc} can quantify the functional activity of ENaC (Sariban-Sohraby and Benos, 1986). In addition, an increase in subunit abundance does not always indicate an increase in functional activity of the whole protein (Sardella and Kültz, 2009; Reilly et al., 2011). For example, the ENaC subunits (α-, β- and γ-subunits) alone cannot induce amiloride-sensitive currents (Canessa et al., 1994), and in bullfrog (*Rana catesbeiana*) tadpoles, ENaC is expressed in the skin but not in a functional state (no amiloride-blockable Na^+ transport present) until metamorphosis (Takada et al., 2006).

Combined with the increase in I_{sc} consistent with an increase in active ion transport, *R. marina* appears to increase NKA and ENaC protein abundance to compensate for Na^+ losses incurred during sloughing. The changes in I_{sc} with spontaneous sloughing are also consistent in magnitude with those observed in toads following aldosterone-induced sloughing events (Nielsen, 1969; Larsen, 1971a; Denèfle et al., 1983), suggesting that the suite of physiological changes that accompany sloughing in amphibians is preserved regardless of whether the sloughing event is initiated naturally or via exogenous hormonal stimulation.

While the sloughing-induced disruption to skin ionoregulatory function in *R. marina* was relatively brief, amphibians display a wide range of sloughing frequencies (Ohmer, 2016) and the net impact of sloughing on physiological homeostasis may be greater in species that slough more frequently. For example, toads in this study sloughed about every 12 days, but some species of amphibians slough as often as every 24 h (Bouwer et al., 1953; Castanho and de Luca, 2001; Ohmer, 2016). In these frequently sloughing species, disruptions to ion and water exchange during sloughing are likely to require a greater energetic investment to maintain ionic and osmotic homeostasis, which cumulatively may represent a significant cost to the animal. In addition, exogenous factors, both biotic and abiotic, that alter sloughing frequency may increase or decrease the overall impact of sloughing on physiological homeostasis. For example, increased sloughing frequency has been observed in amphibians suffering from the devastating disease chytridiomycosis (Ohmer et al., 2015). Chytridiomycosis, a novel and often fatal cutaneous disease of amphibians caused by the fungus *Batrachochytrium dendrobatidis* (*Bd*), appears to disrupt electrolyte transport across the skin of infected frogs (Voyles et al., 2007, 2012). Green tree frogs (*Litoria caerulea*), infected with *Bd* slough as much as 25% more frequently than uninfected frogs (Ohmer et al., 2015) and many other amphibian species are reported to slough more frequently when infected with *Bd*, though the evidence for this is largely anecdotal (Berger et al., 1998; Davidson et al., 2003; Meyer et al., 2012). While an increased sloughing rate may assist with removing pathogens from the skin of infected animals (Meyer et al., 2012; Cramp et al., 2014), sloughing also causes a temporary disruption of ionic and osmotic movements, which, if sloughing frequency is increased, may contribute to the fatal loss of internal ionic homeostasis in clinically infected frogs (Voyles et al., 2009). Thus, future studies that integrate the physiology of sloughing with *Bd* infection are required to more fully understand the mechanistic basis for the morbidity associated with cutaneous *Bd* infection.

Acknowledgements

We would like to thank Prof. M. Grosell (University of Miami) and Dr C. R. Campbell (University of Sydney) for advice on the Ussing chamber protocol. We would also like to thank the UQ School of Biomedical Sciences histology staff for advice on histological procedures, and all volunteers who assisted with animal care and maintenance.

Competing interests

The authors declare no competing or financial interests.

Author contributions
Conceptualization: N.C.W., R.L.C., C.E.F.; Methodology: N.C.W., R.L.C., C.E.F.; Software: N.C.W.; Validation: N.C.W., R.L.C., C.E.F.; Formal analysis: N.C.W.; Investigation: N.C.W.; Resources: N.C.W., R.L.C., C.E.F.; Data curation: N.C.W.; Writing - original draft: N.C.W.; Writing - review & editing: N.C.W., R.L.C., C.E.F.; Visualization: N.C.W.; Supervision: R.L.C., C.E.F.; Project administration: R.L.C., C.E.F.; Funding acquisition: C.E.F.

Funding
This research was funded by an Australian Postgraduate Award (APA) awarded to N.C.W., and a University of Queensland grant awarded to C.E.F.

Supplementary information
Supplementary information available online at
http://jeb.biologists.org/lookup/doi/10.1242/jeb.151738.supplemental

References

Anantharam, A., Tian, Y. and Palmer, L. G. (2006). Open probability of the epithelial sodium channel is regulated by intracellular sodium. *J. Physiol.* **574**, 333-347.
Bentley, P. J. (2002). The Amphibia. In *Endocrines and Osmoregulation: A Comparative Account in Vertebrates*, Vol. 39, pp. 155-186:, Berlin. Heidelberg: Springer-Verlag.
Berger, L., Speare, R., Daszak, P., Green, D. E., Cunningham, A. A., Goggin, C. L., Slocombe, R., Ragan, M. A., Hyatt, A. D., McDonald, K. R. et al. (1998). Chytridiomycosis causes amphibian mortality associated with population declines in the rain forests of Australia and Central America. *Proc. Natl. Acad. Sci.* **95**, 9031-9036.
Boutilier, R. G., Stiffler, D. F. and Toews, D. P. (1992). Exchange of respiratory gases, ions, and water in amphibious and aquatic amphibians. In *Environmental Physiology of the Amphibians* (ed. M. E. Feder and W. W. Burggren). Chicago, USA: University of Chicago Press.
Bouwer, S., Ewer, D. W. and Shiff, C. (1953). Frequency of moulting in Anura. *Nature* **172**, 408.
Budtz, P. E. (1977). Aspects of moulting in anurans and its control. *Symp. Zool. Soc. Lond.* **39**, 317-334.
Budtz, P. E. and Larsen, L. O. (1973). Structure of the toad epidermis during the moulting cycle. I. Light microscopic observations in *Bufo bufo* (L.). *Z. Zellforsch. Mik. Ana.* **144**, 353-368.
Budtz, P. E. and Larsen, L. O. (1975). Structure of the toad epidermis during the moulting cycle. II. Election microscope observations on *Bufo bufo* (L.). *Cell Tissue Res.* **159**, 459-483.
Canessa, C. M., Schild, L., Buell, G., Thorens, B., Gautschi, I., Horisberger, J.-D. and Rossier, B. C. (1994). Amiloride-sensitive epithelial Na+ channel is made of three homologous subunits. *Nature* **367**, 463-467.
Castanho, L. M. and de Luca, I. M. S. (2001). Moulting behavior in leaf-frogs of the genus *Phyllomedusa* (Anura: Hylidae). *Zool. Anz.* **240**, 3-6.
Chuong, C., Nickoloff, B., Elias, P., Goldsmith, L., Macher, E., Maderson, P., Sundberg, J., Tagami, H., Plonka, P. and Thestrup-Pederson, K. (2002). What is the 'true' function of skin? *Exp. Dermatol.* **11**, 159-187.
Crabbé, J. and de Weer, P. (1964). Action of aldosterone on the bladder and skin of the toad. *Nature* **202**, 298-299.
Cramp, R. L., McPhee, R. K., Meyer, E. A., Ohmer, M. E. and Franklin, C. E. (2014). First line of defence: the role of sloughing in the regulation of cutaneous microbes in frogs. *Conserv. Physiol.* **2**, cou012.
Cumming, G., Fidler, F. and Vaux, D. L. (2007). Error bars in experimental biology. *J. Cell Biol.* **177**, 7-11.
Davidson, E. W., Parris, M., Collins, J. P., Longcore, J. E., Pessier, A. P. and Brunner, J. (2003). Pathogenicity and transmission of chytridiomycosis in tiger salamanders (*Ambystoma tigrinum*). *Copeia* **2003**, 601-607.
Denèfle, J.-P., Goudeau, H. and Lechaire, J.-P. (1983). Influence of a transepithelial NaCl gradient on the moulting cycle, keratinization and active sodium transport of isolated frog skin cultured with or without aldosterone. *Roux's Arch. Dev. Biol.* **192**, 234-247.
Eaton, D. C., Malik, B., Saxena, N. C., Al-Khalili, O. and Yue, G. (2001). Mechanisms of Aldosterone's action on epithelial Na+ transport. *J. Membr. Biol.* **184**, 313-319.
Elias, H. and Shapiro, J. (1957). Histology of the skin of some toads and frogs. *Am. Mus. Novit.* **1819**, 1-27.
Erlij, D. and Ussing, H. H. (1978). Transport across amphibian skin. In *Membrane Transport in Biology Vol. 3. Transport Across Multi-Membrane Systems*, Vol. 3 (ed. G. Giebisch, D. C. Tosteson and H. H. Ussing), pp. 175-208. Berlin: Springer-Verlag.
Ernst, V. V. (1973). The digital pads of the tree frog, *Hyla cinerea*. I. The epidermis. *Tissue Cell* **5**, 83-96.
Ewer, R. F. (1951). Water uptake and moulting in *Bufo regularis* Reuss. *J. Exp. Biol.* **28**, 369-373.
Farquhar, M. G. and Palade, G. E. (1964). Functional organization of amphibian skin. *Proc. Natl. Acad. Sci. USA* **51**, 569.
Feder, M. E. and Burggren, W. W. (1992). *Environmental Physiology of the Amphibians*. Chicago, USA: University of Chicago Press.
Garty, H. (1986). Mechanisms of aldosterone action in tight epithelia. *J. Membr. Biol.* **90**, 193-205.
Heatwole, H., Barthalmus, G. T. and Heatwole, A. Y. (1994). *Amphibian Biology. Vol. 1. The Integument*. NSW, Australia: Surrey Beatty & Sons.
Hillyard, S. D., Viborg, A., Nagai, T. and Hoff, K. S. (2007). Chemosensory function of salt and water transport by the amphibian skin. *Comp. Biochem. Physiol. Part A Mol. Integr. Physiol.* **148**, 44-54.
Hillyard, S. D., Møbjerg, N., Tanaka, S. and Larsen, E. H. (2008). Osmotic and ionic regulation in amphibians. In *Osmotic and Ionic Regulation: Cells and Animals* (ed. D. H. Evans), pp. 367-441. FL, USA: CRC Press.
Jaisser, F., Canessa, C. M., Horisberger, J.-D. and Rossier, B. C. (1992). Primary sequence and functional expression of a novel ouabain-resistant Na, K-ATPase. The beta subunit modulates potassium activation of the Na, K-pump. *J. Biol. Chem.* **267**, 16895-16903.
Jørgensen, C. B. (1949). Permeability of the amphibian skin. II. Effect of moulting of the skin of anurans on the permeability to water and electrolytes. *Acta Physiol. Scand.* **18**, 171-180.
Katz, U. (1978). Changes in ionic conductances and in sensitivity to amiloride during the natural moulting cycle of toad skin (*Bufo viridis*, L.). *J. Membr. Biol.* **38**, 1-9.
Kleyman, T. R., Carattino, M. D. and Hughey, R. P. (2009). ENaC at the cutting edge: regulation of epithelial sodium channels by proteases. *J. Biol. Chem.* **284**, 20447-20451.
Koefoed-Johnson, V. and Ussing, H. H. (1958). The nature of the frog skin potential. *Acta Physiol. Scand.* **42**, 298-308.
Konno, N., Hyodo, S., Yamada, T., Matsuda, K. and Uchiyama, M. (2007). Immunolocalization and mRNA expression of the epithelial Na+ channel α-subunit in the kidney and urinary bladder of the marine toad, *Bufo marinus*, under hyperosmotic conditions. *Cell Tissue Res.* **328**, 583-594.
Krzywinski, M. and Altman, N. (2013). Points of significance: error bars. *Nat. Meth.* **10**, 921-922.
Larsen, E. H. (1970). Sodium transport and D.C. resistance in the isolated toad skin in relation to shedding of the *stratum corneum*. *Acta Physiol. Scand.* **79**, 453-461.
Larsen, E. H. (1971a). Effect of aldosterone and oxytocin on the active sodium transport across the isolated toad skin in relation to loosening of *stratum corneum*. *Gen. Comp. Endocr.* **17**, 543-553.
Larsen, E. H. (1971b). The relative contributions of sodium and chloride ions to the conductance of toad skin in relation to shedding of the *stratum corneum*. *Acta Physiol. Scand.* **81**, 254-263.
Larsen, E. H. (1972). Characteristics of aldosterone stimulated transport in isolated skin of the toad, *Bufo bufo* (L.). *J. Steriod Biochem.* **3**, 111-120.
Larsen, L. O. (1976). Physiology of molting. In *Physiology of the Amphibia*, Vol. 3 (ed. B. Lofts), pp. 53-100. London, UK: Academic Press, Inc.
Larsen, E. H. and Ramløv, H. (2013). Role of cutaneous surface fluid in frog osmoregulation. *Comp. Biochem. Physiol. Part A Mol. Integr. Physiol.* **165**, 365-370.
Lillywhite, H. B. and Maderson, P. F. A. (1988). The structure and permeability of integument. *Am. Zool.* **28**, 945-962.
Ling, J. K. (1972). Adaptive functions of vertebrate molting cycles. *Am. Zool.* **12**, 77-93.
Meyer, E. A., Cramp, R. L., Bernal, M. H. and Franklin, C. E. (2012). Changes in cutaneous microbial abundance with sloughing: possible implications for infection and disease in amphibians. *Dis. Aquat. Org.* **101**, 235-242.
Nielsen, R. (1969). The effect of aldosterone in vitro on the active sodium transport and moulting of the frog skin. *Acta Physiol. Scand.* **77**, 85-94.
Nielsen, R. and Tomilson, R. W. S. (1970). The effect of amiloride on sodium transport in the normal and moulting frog skin. *Acta Physiol. Scand.* **79**, 238-243.
Niessen, C. M. (2007). Tight junctions/adherens junctions: basic structure and function. *J. Invest. Dermatol.* **127**, 2525-2532.
Ohmer, M. E. (2016). Interactions between amphibian skin sloughing and a cutaneous fungal disease: infection progression, immune defence, and phylogenetic patterns. *PhD Thesis*, School of Biological Sciences, The University of Queensland.
Ohmer, M. E. B., Cramp, R. L., White, C. R. and Franklin, C. E. (2015). Skin sloughing rate increases with chytrid fungus infection load in a susceptible amphibian. *Funct. Ecol.* **29**, 674-682.
Pfaffl, M. W. (2001). A new mathematical model for relative quantification in real-time RT–PCR. *Nucleic Acids Res.* **29**, e45.
Proksch, E., Brandner, J. M. and Jensen, J.-M. (2008). The skin: an indispensable barrier. *Exp. Dermatol.* **17**, 1063-1072.
Reilly, B. D., Cramp, R. L., Wilson, J. M., Campbell, H. A. and Franklin, C. E. (2011). Branchial osmoregulation in the euryhaline bull shark, *Carcharhinus leucas*: a molecular analysis of ion transporters. *J. Exp. Biol.* **214**, 2883-2895.
Ruhr, I. M., Bodinier, C., Mager, E. M., Esbaugh, A. J., Williams, C., Takei, Y. and Grosell, M. (2014). Guanylin peptides regulate electrolyte and fluid transport in the Gulf toadfish (*Opsanus beta*) posterior intestine. *Am. J. Physiol. Regul. Integr. Comp. Physiol.* **307**, R1167-R1179.

Sardella, B. A. and Kültz, D. (2009). Osmo-and ionoregulatory responses of green sturgeon (*Acipenser medirostris*) to salinity acclimation. *J. Comp. Physiol. B* **179**, 383-390.
Sariban-Sohraby, S. and Benos, D. (1986). The amiloride-sensitive sodium channel. *Am. J. Physiol. Cell Physiol.* **250**, C175-C190.
Shoemaker, V. H., Hillman, S. S., Hillyard, S. D., Jackson, D. C., Mc Clanahan, L. L., Jr, Withers, P. C. and Wygoda, M. L. (1992). Exchange of water, ions, and respiratory gases in terrestrial amphibians. In *Environmental Physiology of the Amphibians*, (ed. M. E. Feder and W. W. Burggren). Chicago, USA: University of Chicago Press.
Smith, P. G. (1975). Aldosterone-induced moulting in amphibian skin and its effect on electrical capacitance. *J. Membr. Biol.* **22**, 165-181.
Takada, M., Shimomura, T., Hokari, S., Jensik, P. J. and Cox, T. C. (2006). Larval bullfrog skin expresses ENaC despite having no amiloride-blockable transepithelial Na+ transport. *J. Comp. Physiol. B* **176**, 287-293.
Thorson, T. B. (1964). The partitioning of body water in amphibia. *Physiol. Zool.* **37**, 395-399.
Tsukita, S., Furuse, M. and Itoh, M. (2001). Multifunctional strands in tight junctions. *Nat. Rev. Mol. Cell Biol.* **2**, 285-293.
Ussing, H. H. and Zerahn, K. (1951). Active transport of sodium as the source of electric current in the short-circuited isolated frog skin. *Acta Physiol. Scand.* **23**, 110-127.
Voyles, J., Berger, L., Young, S., Speare, R., Webb, R., Warner, J., Rudd, D., Campbell, R. and Skerratt, L. F. (2007). Electrolyte depletion and osmotic imbalance in amphibians with chytridiomycosis. *Dis. Aquat. Org.* **77**, 113-118.
Voyles, J., Young, S., Berger, L., Campbell, C., Voyles, W. F., Dinudom, A., Cook, D., Webb, R., Alford, R. A., Skerratt, L. F. et al. (2009). Pathogenesis of chytridiomycosis, a cause of catastrophic amphibian declines. *Science* **326**, 582-585.
Voyles, J., Vredenburg, V. T., Tunstall, T. S., Parker, J. M., Briggs, C. J. and Rosenblum, E. B. (2012). Pathophysiology in mountain yellow-legged frogs (*Rana muscosa*) during a chytridiomycosis outbreak. *PLoS ONE* **7**, e35374.
Whitear, M. (1975). Flask cells and epidermal dynamics in frog skin. *J. Zool.* **175**, 107-149.

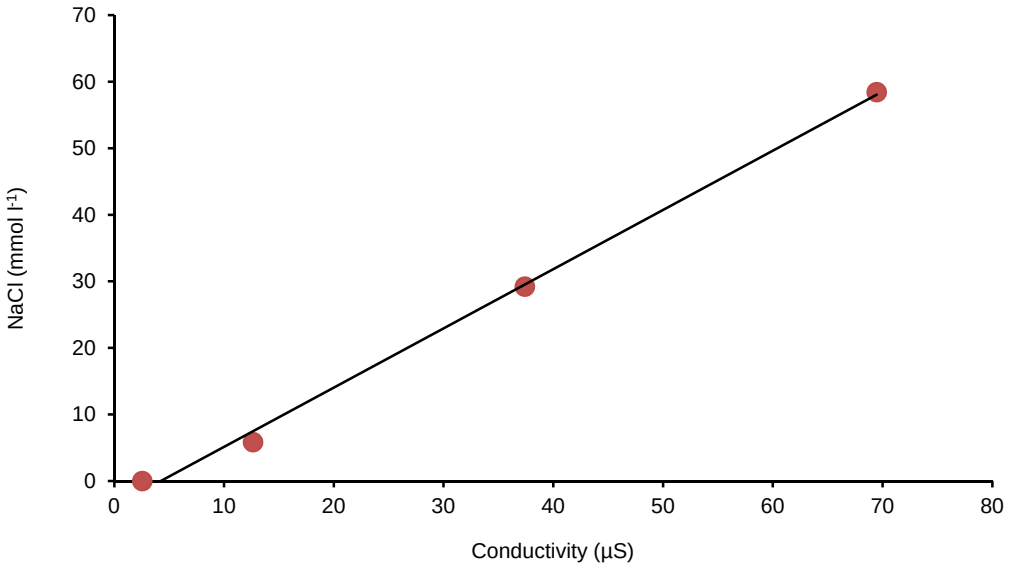

Fig. S1. Relationship between conductivity readings (G, µS) and known NaCl (c_i, mmol l^{-1}) concentrations show a predicable linear relationship (c_i = 0.015 x G - 0.064, r^2 = 0.99).

The RO only solution and solutions where the animal was in the intermoult phase did not have any detectable sodium or potassium.

Journal of Experimental Biology • Supplementary information